

# ANALYSIS NOISE, SHORT-BASELINE TIME TRANSFER, AND A LONG-BASELINE GPS CARRIER-PHASE FREQUENCY SCALE

Demetrios N. Matsakis, Ken Senior, and Lee A. Breakiron  
U.S. Naval Observatory  
Washington, DC 20392, USA

## Abstract

*The calibrated carrier-phase GPS technique promises time transfer between remote sites with 5-minute precision approaching 20 ps. Uncalibrated time transfers between many sites are routinely made available by the Earth Orientation Department of the U.S. Naval Observatory (USNO). Although important technical issues involving long-term accuracy and calibration are still being resolved, it is possible to generate sample time and frequency scales so as to anticipate the full power of the technique. Using minor extensions of the USNO's postprocessed extended-Percival algorithm SuperP [1], a carrier-phase-based frequency scale is generated and compared to local USNO timescales.*

## INTRODUCTION

The U.S. Naval Observatory (USNO) is actively pursuing the concept of a "Distributed Master Clock," which would use GPS carrier-phase data to provide on-line timing ensembling and synchronization of many remote sites. It is anticipated that easily incorporated improvements to the services currently provided by the Analysis Centers of the International GPS Service (IGS) would prove adequate for this purpose. Among the required improvements would be the use of calibrated and calibratable GPS receivers [2] and the elimination of solution day-boundary discontinuities. Although these improvements are all necessary or important for time transfer, they do not obviate frequency transfer, or the generation of frequency scales. We of course do not wish to trivialize the difficulties or the practical importance of being able to integrate a frequency scale to a timescale; this work should therefore be considered a progress report on efforts to assess the promise of the carrier-phase technique.

## DATA REDUCTION

The input data for this analysis were obtained from the daily reductions of carrier-phase data routinely produced by the USNO's Earth Orientation (EO) Department, and initially included 47 sites whose timing reference was listed as a maser in their site logs, as listed by the IGS with URL <http://igscb.jpl.nasa.gov/network/site>. The data were taken from MJD 51062 through 51384 (6 Sep 98-25 Jul 99). Timing data from the IGS sites designated USNO (located at our Washington, DC, site) and AMC1 and AMC2 (located at the USNO's Alternate Master Clock at Schriever AFB in Colorado) were automatically corrected for the TurboRogue receivers'

Report Documentation Page				Form Approved OMB No. 0704-0188	
Public reporting burden for the collection of information is estimated to average 1 hour per response, including the time for reviewing instructions, searching existing data sources, gathering and maintaining the data needed, and completing and reviewing the collection of information. Send comments regarding this burden estimate or any other aspect of this collection of information, including suggestions for reducing this burden, to Washington Headquarters Services, Directorate for Information Operations and Reports, 1215 Jefferson Davis Highway, Suite 1204, Arlington VA 22202-4302. Respondents should be aware that notwithstanding any other provision of law, no person shall be subject to a penalty for failing to comply with a collection of information if it does not display a currently valid OMB control number.					
1. REPORT DATE <b>DEC 1999</b>		2. REPORT TYPE		3. DATES COVERED <b>00-00-1999 to 00-00-1999</b>	
4. TITLE AND SUBTITLE <b>Analysis Noise, Short-Baseline Time Transfer, and a Long-Baseline GPS Carrier-Phase Frequency Scale</b>				5a. CONTRACT NUMBER	
				5b. GRANT NUMBER	
				5c. PROGRAM ELEMENT NUMBER	
6. AUTHOR(S)				5d. PROJECT NUMBER	
				5e. TASK NUMBER	
				5f. WORK UNIT NUMBER	
7. PERFORMING ORGANIZATION NAME(S) AND ADDRESS(ES) <b>U.S. Naval Observatory, Washington, DC, 20392</b>				8. PERFORMING ORGANIZATION REPORT NUMBER	
9. SPONSORING/MONITORING AGENCY NAME(S) AND ADDRESS(ES)				10. SPONSOR/MONITOR'S ACRONYM(S)	
				11. SPONSOR/MONITOR'S REPORT NUMBER(S)	
12. DISTRIBUTION/AVAILABILITY STATEMENT <b>Approved for public release; distribution unlimited</b>					
13. SUPPLEMENTARY NOTES <b>See also ADM001481. 31st Annual Precise Time and Time Interval (PTTI) Planning Meeting, 7-9 December 1999, Dana Point, CA</b>					
14. ABSTRACT <b>see report</b>					
15. SUBJECT TERMS					
16. SECURITY CLASSIFICATION OF:			17. LIMITATION OF ABSTRACT <b>Same as Report (SAR)</b>	18. NUMBER OF PAGES <b>14</b>	19a. NAME OF RESPONSIBLE PERSON
a. REPORT <b>unclassified</b>	b. ABSTRACT <b>unclassified</b>	c. THIS PAGE <b>unclassified</b>			

internal delay jumps using the procedures outlined in [3], but this made little difference as the timing data were then replaced by their first differences (frequencies) that were then edited for outliers. Day-boundary discontinuities were avoided by excluding frequencies generated from data that spanned those boundaries, and only reductions in which the USNO receiver was used as a reference were utilized. Outlier-removal algorithms eliminated all single-point fluctuations in excess of 15 “deviations,” where one “deviation” is defined to be half the difference between the frequency exceeded by 84% of the data minus the frequency exceeded by 16% of the data (so that the “deviation” is to the standard deviation as the median is to the average).

The clock data, in the form of estimated and edited frequency differences between the USNO and site receivers, were then input into the USNO program SuperP for clock characterization [1]. This program applies a postprocessed Percival-type algorithm which computes the instrumental frequency bias and drift of all clocks relative to one fiducial clock via least squares. Data from clocks whose frequency or rate seemed to shift suddenly to a new value, relative to the USNO reference, were treated as if from a different clock. The time reference for the USNO receiver is Master Clock #3 (MC3), and is referred to as the “USNO reference” because it was only used as a reference, and has no influence on the clock characterization or the subsequent averaging for the generation of a frequency scale. The absolute frequency and frequency drift biases of the fiducial clock cannot be determined from clock differences; however, for the purpose of data editing they were chosen so as to keep the average of individual clock frequencies and drifts close to the USNO reference. Because these assumptions and this procedure result in an undetermined overall rate and drift shift in the frequency scales produced, the standard “ $\sigma_y$ ” analysis has been supplemented with the “ $\sigma_z$ ” statistic [4,5], which is independent of both rate and drift. Both these measures were generalized slightly, as appropriate, to allow for the fact that the data are unevenly spaced and expressed in terms of frequency instead of phase.

It was found that outlier removal on the basis of individual 5-minute frequency points was insufficient to identify all incorrect data, as there were times when sequences of obviously erroneous frequencies would be revealed only after the data were averaged into hourly or half-day bins. In some cases, the site logs showed that these variations were related to maser tuning or repair; however, at other times there was no such indication. Although we anticipate that at some point the IGS will stipulate that clock records be systematically maintained and made publicly available, there will always be unexpected frequency excursions related to hardware or software failures. For this work, outlier removal was completed by a manual iterative process in which SuperP-corrected clock data were inspected, and then new clock characterizations generated on edited data. Clocks whose frequencies showed significantly higher variance or extreme non-white behavior were excluded completely, so that in the end only data that were used came from the following 14 IGS sites: ALGO, AMC, DRAO, FAIR, GODE, HOB2, HRAO, KOKB, MATE, MKEA, NLIB, NRC1, PIE1, and USNO. Figure 1 shows how many sites contributed to the final frequency scales at any one time.

One potentially serious issue is that for some sites we were not able to obtain information concerning clock steering. Although the SuperP algorithm’s implementation should remove the effects of large, sudden changes, any clocks being smoothly steered to UTC would simply appear to be very good clocks over the long term. However, since the USNO unsteered maser mean timescale (UNSTMM) is probably more frequency stable than UTC over the time range of interest (due to the noise of common-view time transfer being folded into UTC), any unmodeled steering of IGS site clocks would tend to weaken the conclusions of this paper, and proper allowance for such steering would strengthen them.

For clock characterization, fits were made to frequency differences between each pair of clocks, and points were weighted by the inverse of their squared formal errors, as computed statistically

assuming the error values output by GIPSY were uncorrelated. It was found that essentially the same results were achieved using unit weights for clock characterization.

## THE FREQUENCY SCALE

Once the iterative process of clock characterization was complete, detrended clock frequencies were averaged into 3-hour bins. This was necessary to make the subsequent average less sensitive to the intermittent loss of data that have a bias. Not surprisingly, for data massaged so as to maximize their “whiteness,” it was found that weighting data by their inverse variances produced a closer match between the individual clock frequencies and the scale than did unit-weighting. However, it also produced a closer match between the frequency scale and the UNSTMM, which played no role in the frequency scale generation (nor did any of the USNO masers). Figure 2 shows that the frequency scale was closer to our UNSTMM than to USNO MC3 (steered to the USNO Master Clock, which in turn is steered to UTC), and from this we conclude that the frequency scale derived from IGS data is meaningful.

Figure 3 displays the  $\sigma_y$  plots associated with the scales in Figure 2. A frequency drift was removed from these plots, which forces each curve to negative infinity for large  $\tau$ .

Figure 4 displays  $\sigma_z$  plots with the scales of Figure 2.  $\sigma_z$  can be considered a generalization of the Hadamard variance for unequally spaced data.

Figure 5 compares  $\sigma_y$  plots of individual IGS sites, using the IGSFS as a reference, with the  $\sigma_y$  plots of the local USNO masers, using the UNSTMM as a reference, and Figure 6 uses the  $\sigma_z$  statistic for the same data.

## FREQUENCY TRANSFER TO THE USNO ALTERNATE MASTER CLOCK (AMC)

Data from the USNO AMC were not included in the frequency scale analysis because its master clock is steered to UTC(USNO) and we wished to avoid even the suspicion of adding pre-correlated data. However, the AMC is uniquely qualified to serve as a time-transfer test bed due to its large ensemble of clocks and the hourly time transfers with USNO-DC via calibrated Two-Way Satellite Time Transfer (TWSTT).

Figures 7 and 8 display the  $\sigma_y$  and  $\sigma_z$  plots of the differences between the UNSTMM (unsteered average of up to 10 masers at USNO-DC) with the unsteered average of the two masers at the USNO AMC when frequency (or time) transfer is achieved via carrier-phase, P-code common-view GPS, and TWSTT. Common-view data are from 48-hour linear fits to 13-minute single-channel, dual-frequency observations. The downconverter in the AMC GPS receiver's antenna was improved subsequent to this, and more recent data indicate a performance better by about .25 in logarithmic units.

## OCCASIONALLY IGNORED TIME-TRANSFER ISSUES

The primary problem in implementing carrier-phase time transfer is for calibrated and calibratable receive systems, which are both environmentally protected and environmentally insensitive, such as the Geodetic Time Transfer receivers (GeTT, designated USNB in the data reduction)

[6]. Herein we discuss two other considerations: carrier-phase data-analysis noise, and errors in ensembling local clocks.

“Analysis noise” is a term loosely used to describe the fact that different researchers or operational centers can compute different time-transfer results between two sites despite using identical data from those sites. This can be due to differences in software, modelling, parameterizing, editing, or use of data from other sites in a combined solution. In order to provide a crude estimate of analysis noise, data reduced by the USNO EO Department using the GIPSY software package were compared to data reduced by the CODE analysis center in Bern, Switzerland, using the Bernese software package. Figure 9 compares double-differenced data from the short-baseline USNO and USNB receivers with data from the 2000-km baseline AMC vs. USNO and AMC vs. USNB. Large excursions are typically associated with high formal errors from the solutions and have been excluded in the figure. Excluding those outliers, we estimate about 1 ns for the peak-to-peak analysis noise in GPS carrier phase.

The largest error in the USNO-DC measurements is due to the mostly underground time transfer between our two buildings, which is realized via the phase of the clock 5 MHz signals (Table 1). Operational data are transferred to Building 78 from Building 52 via fiber optics using an LED light source. Two additional signals are also sent via parallel means: MC3’s signals (in Bldg. 52) are sent through a different set of fiber optics using lasers, and signals from one maser (NAV2) are sent to Bldg. 78 via a coaxial cable. In the reverse direction, lasers are used to send the signal from the USNO MC (MC2, in Bldg. 78) to Bldg. 52. The laser signals are also split at each end so as to be measured via multiple measurement systems, which agree to about 100 ps, peak to peak. Since we also have TWSTT and carrier-phase connections between the two buildings, the USNO-DC is an excellent test bed for short-baseline time transfer.

By differencing the values of MC2-MC3 measured by each signal going to Bldg. 78 to create double-differences, it is possible to measure the relative change in their delay. It is also possible to measure the variations of the total round-trip delay, by differencing MC2-MC3 from the laser-based signals going to Bldg. 78 from those going from Bldg. 78. Figure 10 shows these differences along with the measured temperatures along the path, and Figure 11 compares the same double-differenced delays with the measured relative humidities.

The round-trip differences provide the best measure of the change in delay with temperature, which would tend to cancel for signals going in the same direction. The outdoor temperature appears to be the only significant contributor; some apparent correlations with relative humidity are probably due to associated temperature variations. The temperature of the room in which the time distribution electronics and measurement systems are kept appears to be significant only at times of  $>10^{\circ}\text{F}$  environmental variations due to control equipment failure (which are not shown in the figure). A variable diurnal cycle of roughly 70-150 ps peak-to-peak amplitude is correlated with the time of the exterior daily temperature variations, but not the amplitude (Figure 12). Comparisons of the transmitted signals with those of unsteered clocks at each site show that roughly two-thirds of the round-trip delay is in the line from Bldg. 78 to Bldg. 52, and one-third in the lines from Bldg. 52 to Bldg. 78.

The observed variation is too large to be explained by thermal expansion of the glass: assuming a cable length of 160 m underground and 70 m within buildings, a glass index of refraction of 1.4, a refraction angle correction of 1.2, and a thermal expansion coefficient of  $8.5 \times 10^{-6}/^{\circ}\text{C}$ , one expects a round-trip delay variation of 15 ps/ $^{\circ}\text{C}$  underground and 7 ps/ $^{\circ}\text{C}$  within the buildings. The observed underground seasonal variations of  $22^{\circ}\text{C}$  are an order of magnitude too small to explain the observed 3 ns seasonal variations in round-trip delay. Although these calculations do not include the dielectric constant, they appear to be consistent with previously reported

values of 6-7 ppm/°C [7-9]. In the context of this paper our inability to explain the variation is not important, because we have recently received and plan to install temperature-compensated coaxial cable and fiber optics, and also because the observed associated single-direction delay variations are less than 1 ns peak to peak, and therefore adequate for the purpose of evaluating carrier phase to that level. Figure 13 shows that carrier-phase timing differences measured using receivers USNO (in Bldg. 52) and USNB (the GeTT, in Bldg. 78) show much larger variations, of about 3 ns peak to peak. This is probably all due to errors in the carrier phase technique as currently practiced, and it is interesting that these errors are similar to those in the TWSTT link between the two buildings.

## CONCLUSIONS

We conclude that it is currently possible to generate an excellent frequency scale using GPS carrier-phase data, and anticipate no significant problems in the generation of a timescale, once known technology is actually installed at a sufficient number of sites. Analysis noise is subnanosecond rms, and hardware limitations may be 1 ns rms, ignoring currently serious hardware calibration considerations in our equipment.

## ACKNOWLEDGMENTS

We wish to acknowledge the work of Merri Sue Carter, Chris Ekstrom, Arvid Myers, Jim Ray, Jim Rohde, Tom Swanson, Fred Torcaso, and Paul Wheeler. We also wish to thank Leon Prost, Gregor Duddle, and Frederick Overney of the Swiss Federal Office of Metrology and Thomas Schildknecht and Tim Springer of the Astronomical Institute of the University of Bern for use of their raw and reduced GeTT data.

## REFERENCES

- [1] D. Matsakis, and L. Breakiron 1999, "*A New Postprocessed Algorithm for a Free-Running Timescale and a Comparison with ALGOS and AT1 Algorithms*," Proceedings of the 30th Annual Precise Time and Time Interval (PTTI) Systems and Applications Meeting, 1-3 December 1998, Reston, Virginia, USA, pp 19-34.
- [2] E. Powers 2000, "*Calibration of GPS Carrier-Phase Time-Transfer Equipment*," these Proceedings.
- [3] E. Powers, D. Judge, and D. Matsakis 1999, "*Hardware Delay Measurements and Sensitivities in Carrier Phase Time Transfer*," Proceedings of the 30th Annual Precise Time and Time Interval (PTTI) Systems and Applications Meeting, 1-3 December 1998, Reston, Virginia, USA, pp. 293-305.
- [4] D. Matsakis, J. Taylor, and T. M. Eubanks 1997, "*A Statistic for Describing Pulsar and Clock Stabilities*," *Astronomy and Astrophysics*, **326**, 924.
- [5] D. Matsakis, and F. J. Josties 1997, "*Pulsar-Appropriate Clock Statistics*," Proceedings of the 28th Annual Precise Time and Time Interval (PTTI) Applications and Planning Meeting, 3-5 December 1998, Reston, Virginia, USA, pp. 225-230.
- [6] R. Dach, T. Schildknecht, T. Springer, G. Duddle, and L. Prost 2000, "*Recent Results with Transatlantic GeTT Campaign*," these Proceedings.

- [7] G. Lutes, and A. Kirk 1987, "*Reference Frequency Transmission Over Optical Fiber*," Proceedings of the 18th Annual Precise Time and Time Interval (PTTI) Applications and Planning Meeting, 2-4 December 1986, Reston, Virginia, USA, pp. 385-394.
- [8] J. C. Webber, and D. L. Thacker 1990, "*Phase Distribution on Fiber Optic Cable*," Proceedings of the 21st Annual Precise Time and Time Interval (PTTI) Applications and Planning Meeting, 28-30 November 1989, Redondo Beach, California, USA, pp. 139-144.
- [9] M. Calhoun, and P. Kuhnle 1993, "*Ultrastable Reference Frequency Distribution Utilizing a Fiber Optic Link*," Proceedings of the 24th Annual Precise Time and Time Interval (PTTI) Applications Meeting, 1-3 December 1992, Reston, Virginia, USA, pp. 357-364.

Table 1. USNO-DC Link Between Buildings	
Bldg. 52 MC3 = IGS ref	<-----> Bldg. 78 MC2 = UTC(USNO)
<p>I. 5 MHz signals sent from Bldg. 52 to Bldg. 78</p> <ul style="list-style-type: none"> <li>A. All clocks via LED-based fiber optics</li> <li>B. MC3 via laser-based fiber optics (B - A &lt; 1 ns)</li> <li>C. One maser (NAV2) via RG223 coaxial cable (C - A &lt; 2 ns)</li> <li>D. TWSTT (D - A &lt; 3 ns)</li> <li>E. Carrier-phase (USNO - USNB) (E - A &lt; 3 ns)</li> <li>F. Portable cesium 1-pps (F - A &lt; .5 ns)</li> </ul> <p>(Values in parentheses estimate peak-to-peak differences between each technique and the first).</p> <p>II. 5 MHz signal sent from Bldg. 78 to Bldg. 52 via laser-based fiber optics</p> <p style="text-align: center;">Round Trip-Delay Variations:</p> <p style="text-align: center;">(MC2 - MC3)<sub>Bldg.52</sub> - (MC2 - MC3)<sub>Bldg.78</sub></p> <p style="text-align: center;">Round-Trip Delay &lt; 3 ns (seasonal p/p) &lt; 150 ps (diurnal p/p)</p> <p>C. Temperature-compensated coaxial cables (to be installed)</p>	

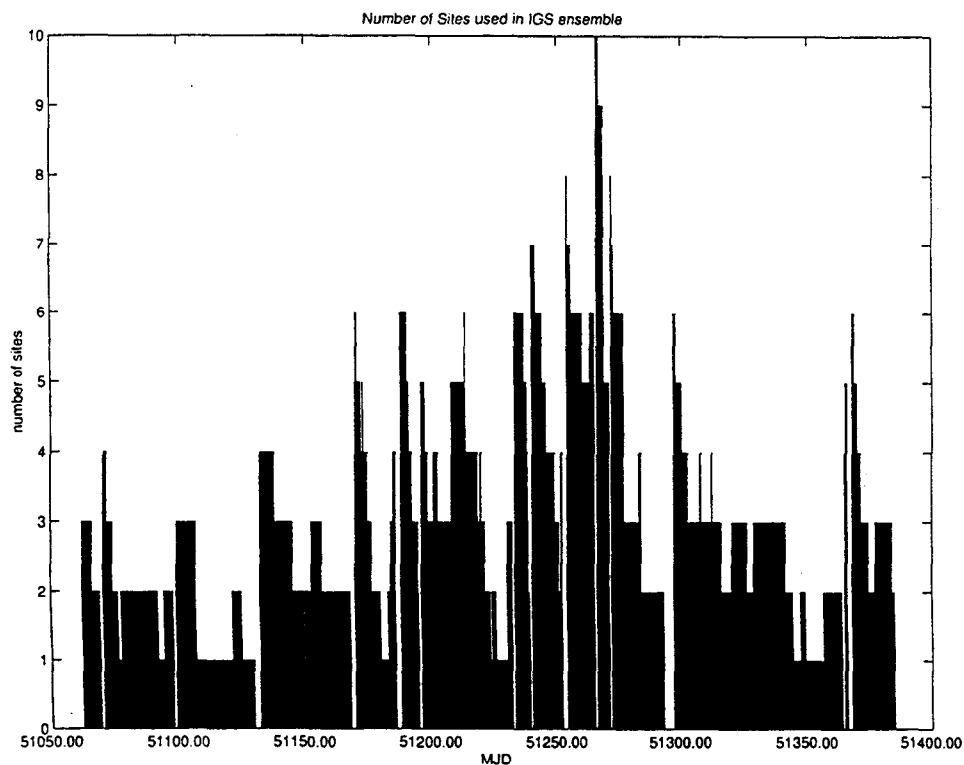


Figure 1. Histogram of number of sites contributing to frequency scale as function of time.

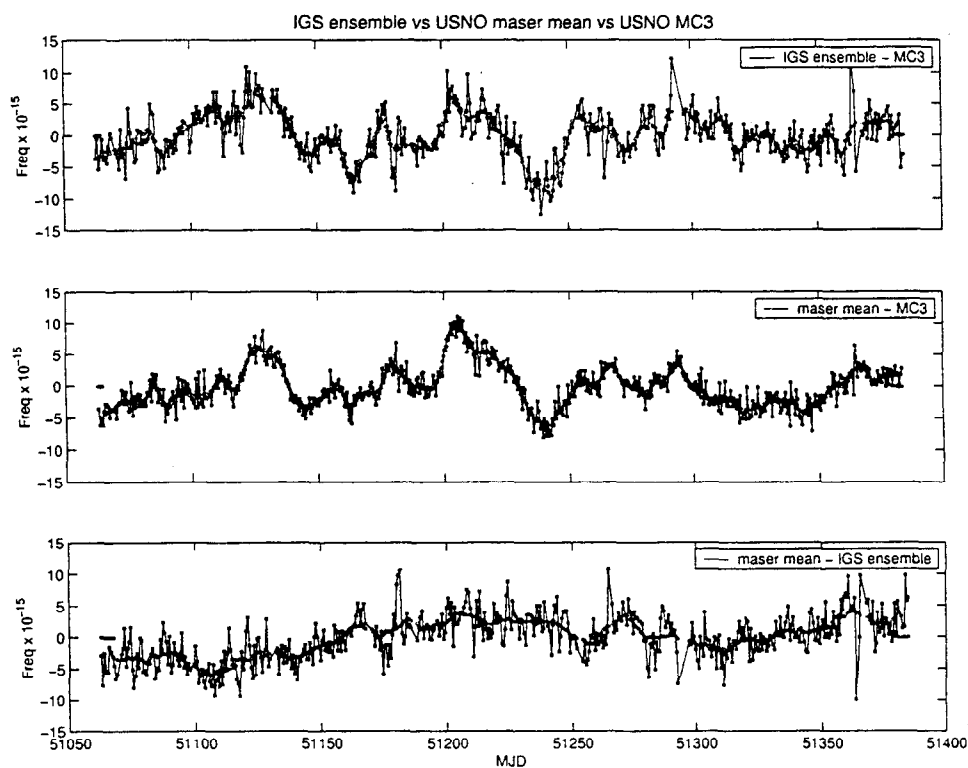


Figure 2. Frequency scales, in units of parts in  $10^{15}$  (fs/s). The top plot is the unsteered USNO maser mean minus the carrier-phase based scale; middle is the unsteered maser mean minus MC3; and bottom is the carrier-phase frequency scale minus MC3.



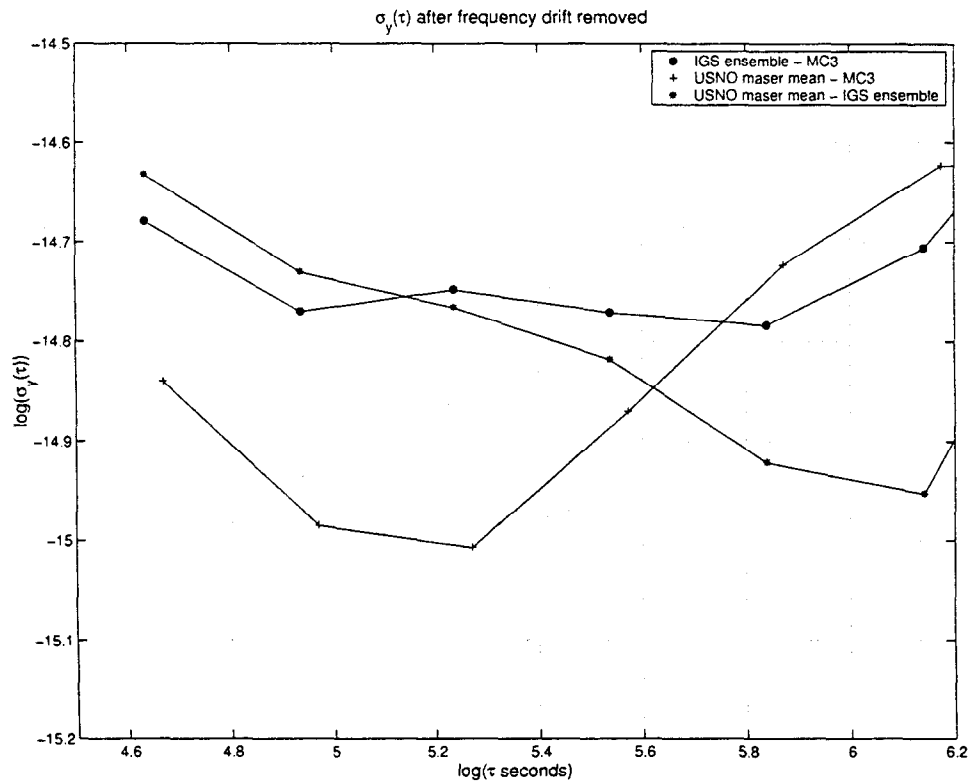


Figure 3.  $\sigma_y$  plots of parabola-removed frequency scales in Figure 2. Symbol 1 is the carrier-phase frequency scale minus MC3; symbol 2 denotes the unsteered maser mean minus Master Clock 3; and symbol 3 denotes the unsteered maser mean minus carrier-phase frequency scale.

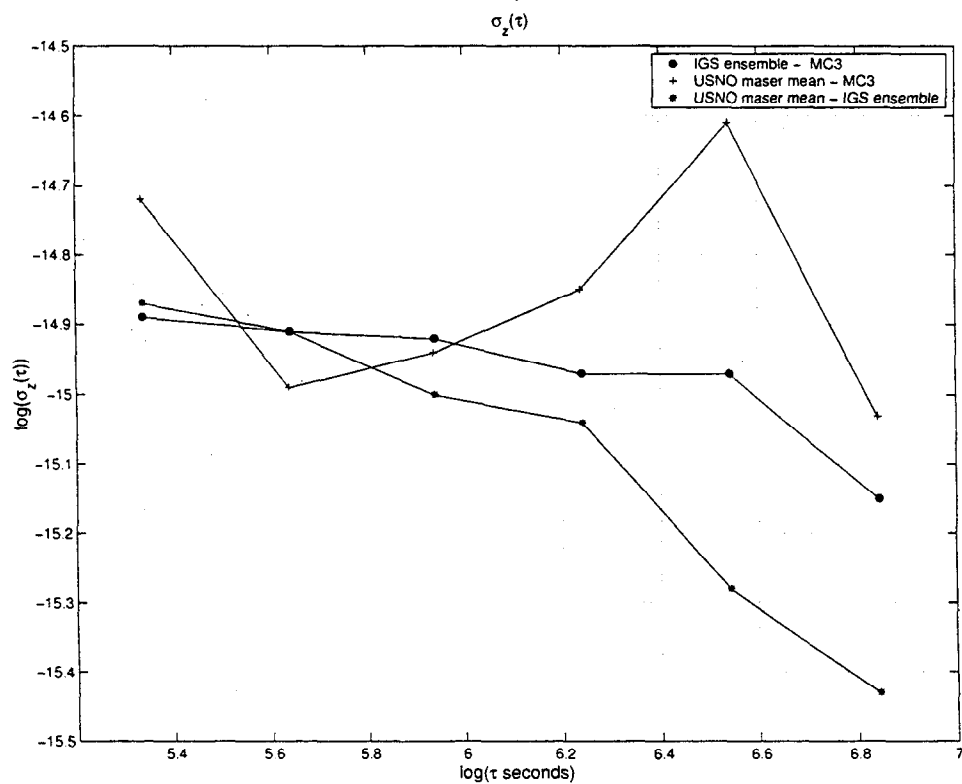


Figure 4.  $\sigma_z$  plots of frequency scale differences; symbols have same significance as in previous figure.

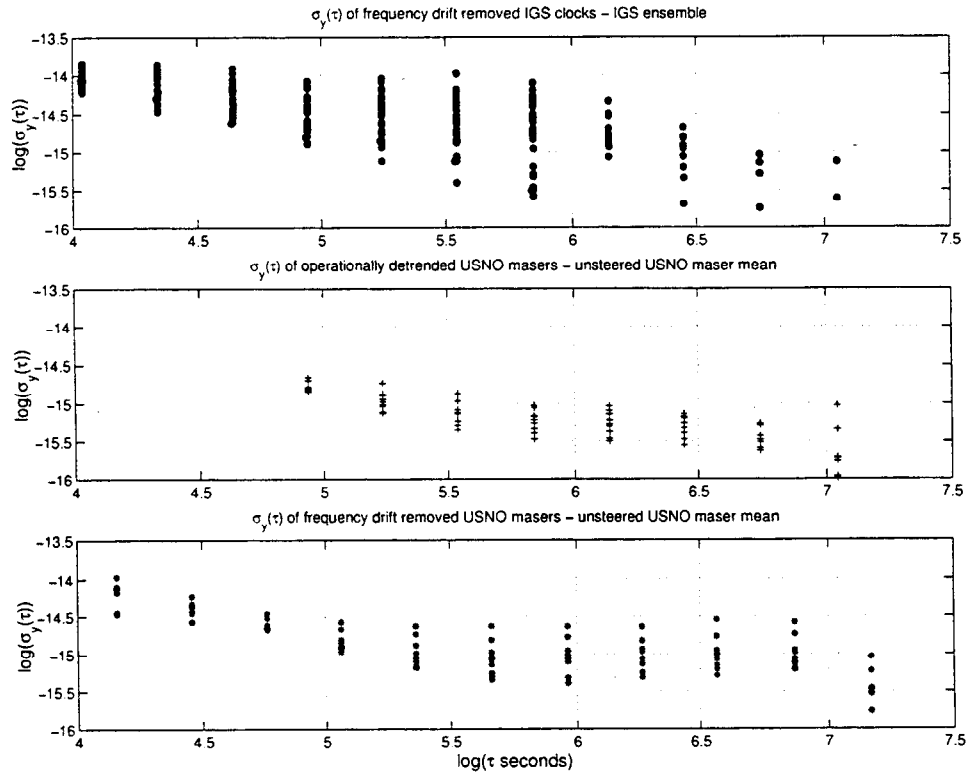


Figure 5. Top:  $\sigma_y$  of each detrended IGS maser, using the IGS frequency scale as a reference. Middle:  $\sigma_y$  of each edited and detrended USNO maser, using the USNO unsteered maser-mean (UNSTMM) as a reference. Bottom:  $\sigma_y$  for uncorrected USNO maser data, using the UNSTMM as a reference.

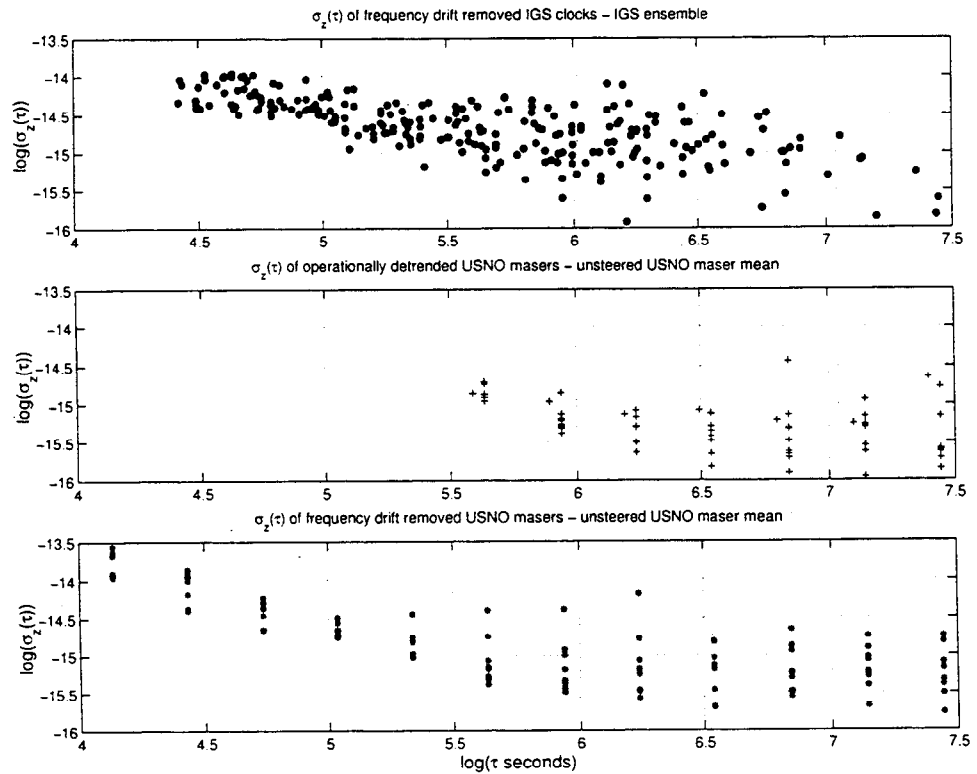


Figure 6. As in previous figure, except the  $\sigma_z$  statistic is applied.

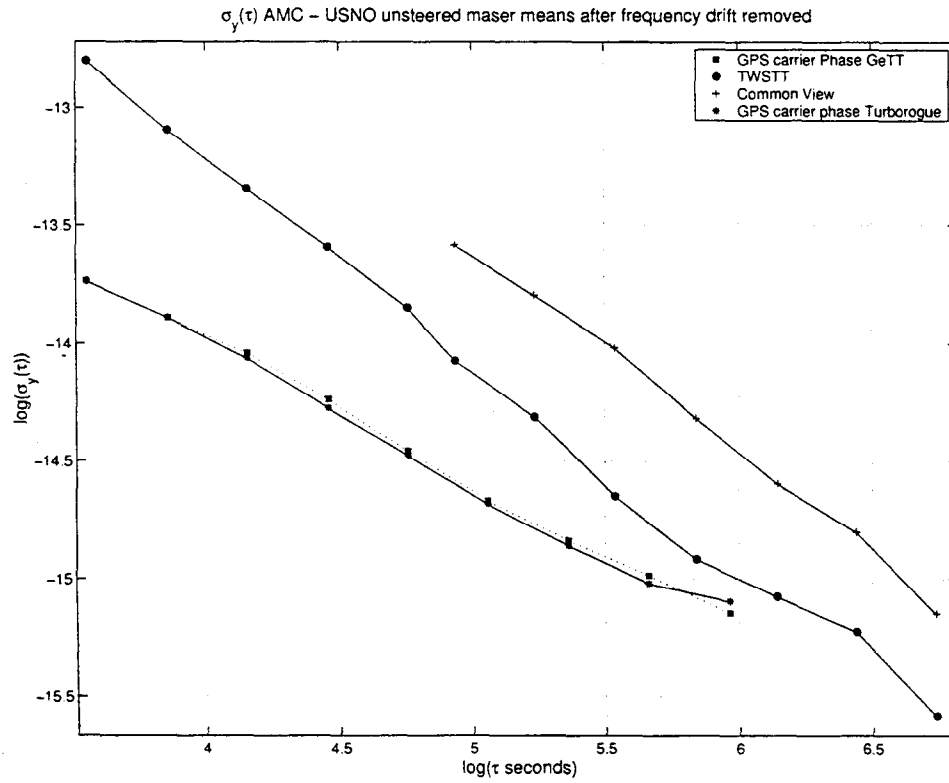


Figure 7.  $\sigma_y$  plots of parabola-removed timing differences between the USNO unsteered maser mean and the average of the two AMC masers. Symbols 1 and 2 use carrier-phase via IGS receivers USNO or USNB; symbol 3 uses dual-frequency P-code GPS common view; and symbol 4 depicts TWSTT.

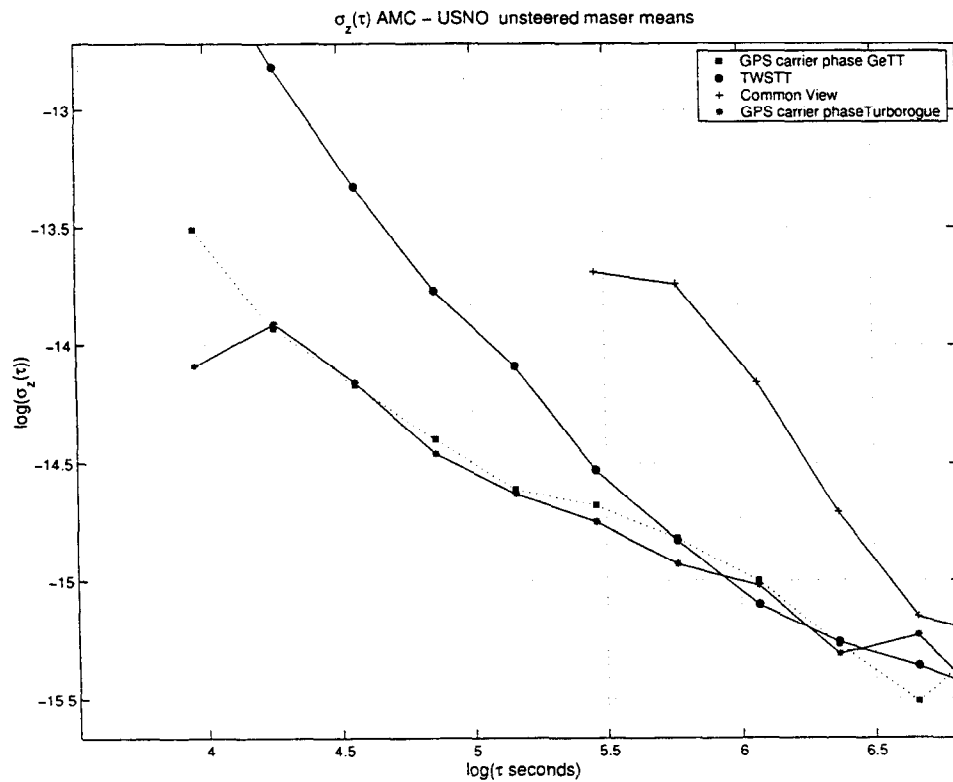


Figure 8. As in previous figure, except  $\sigma_z$  is used instead of  $\sigma_y$ .

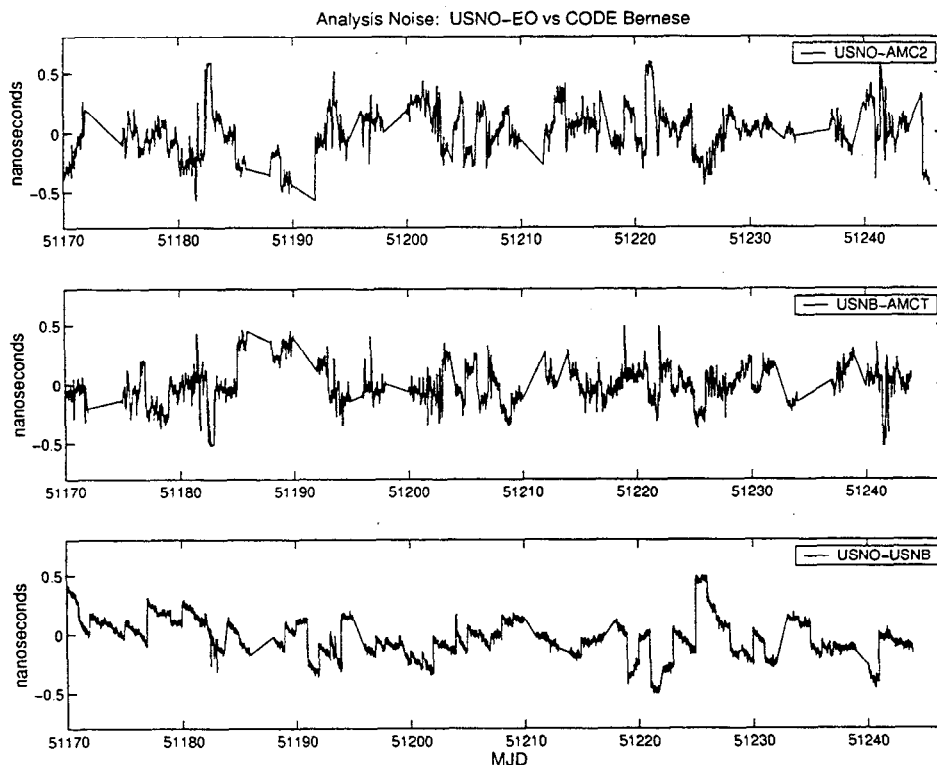


Figure 9. Analysis noise, as measured by differences in solutions generated by USNO and CODE. Top is for baseline USNO-AMC1, and bottom is for USNB-USNO. Very large excursions, not shown, are associated with high formal errors computed by the solution.

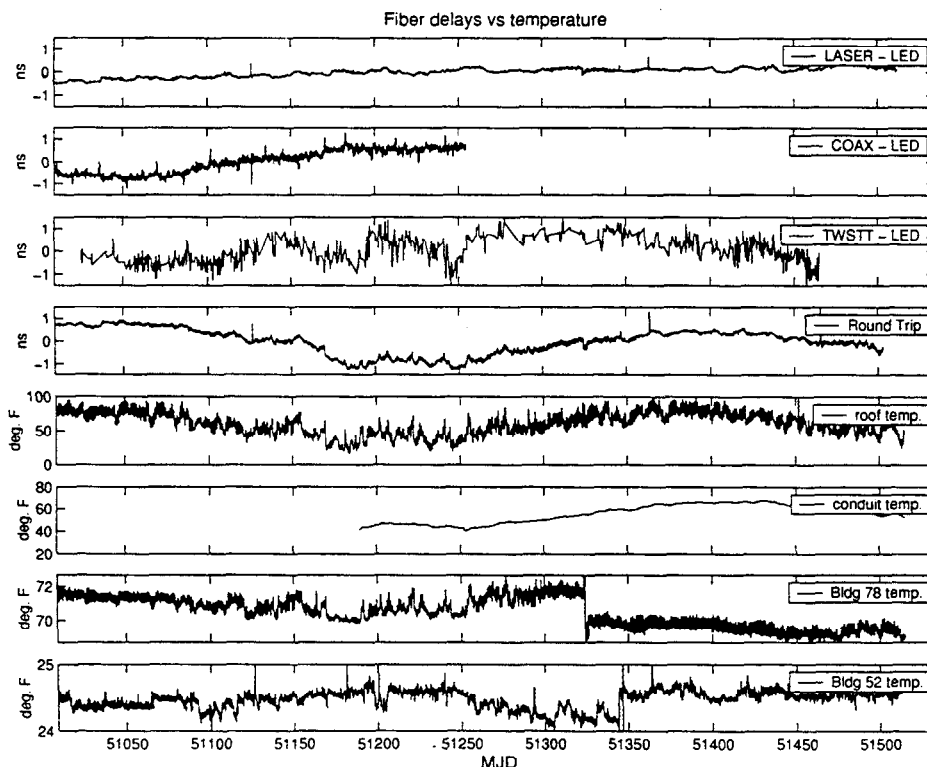


Figure 10. Timing differences between Bldgs. 78 and 52 in USNO-DC in the form of MC2-MC3 measurements subtracted from MC2-MC3 measurements using an LED-based fiber-optic system. The upper three plots, from top to bottom: uncalibrated TWSTT, underground coaxial cable, and laser-based fiber optics. The coaxial-LED double-difference data in the second plot extend back through 4 years to MJD 49800, and show a fairly constant peak-to-peak seasonal variation of 2 ns. The fourth plot is the round-trip delay measured by two laser-links. The lower four plots, from top to bottom: temperatures in the Bldg. 78 measurement room, near an underground tunnel junction, outdoors, and in the Bldg. 52 measurement room.

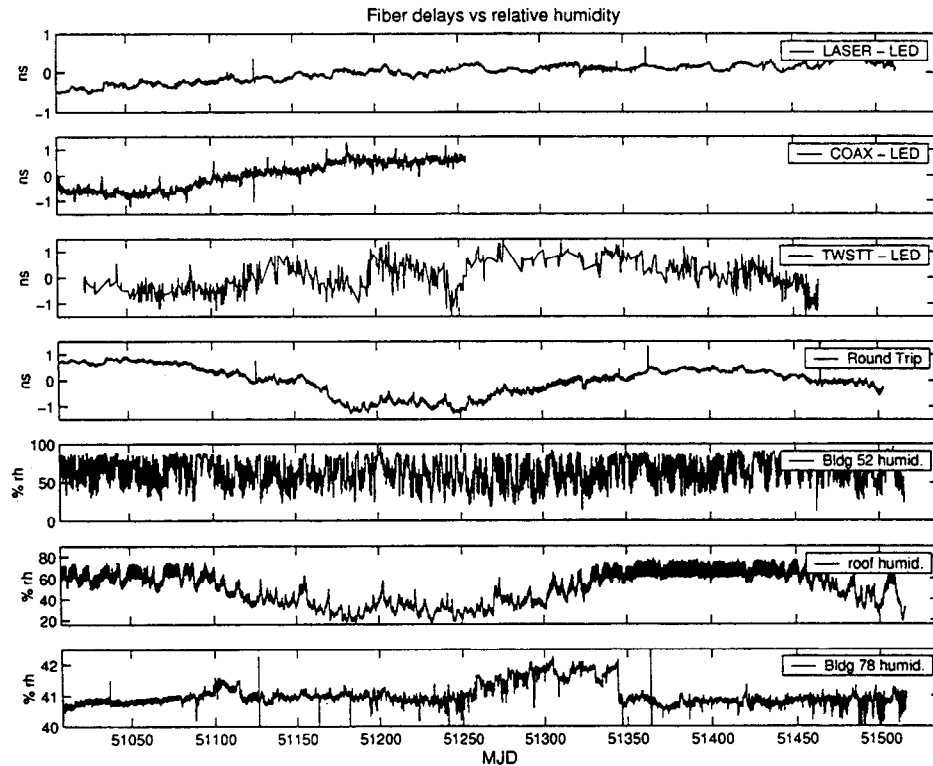


Figure 11. The upper four plots are the same timing differences as in Figure 10. The lower three plots, from top to bottom: relative humidity of the Bldg. 78 measurement room, outdoors, and the Bldg. 52 measurement room.

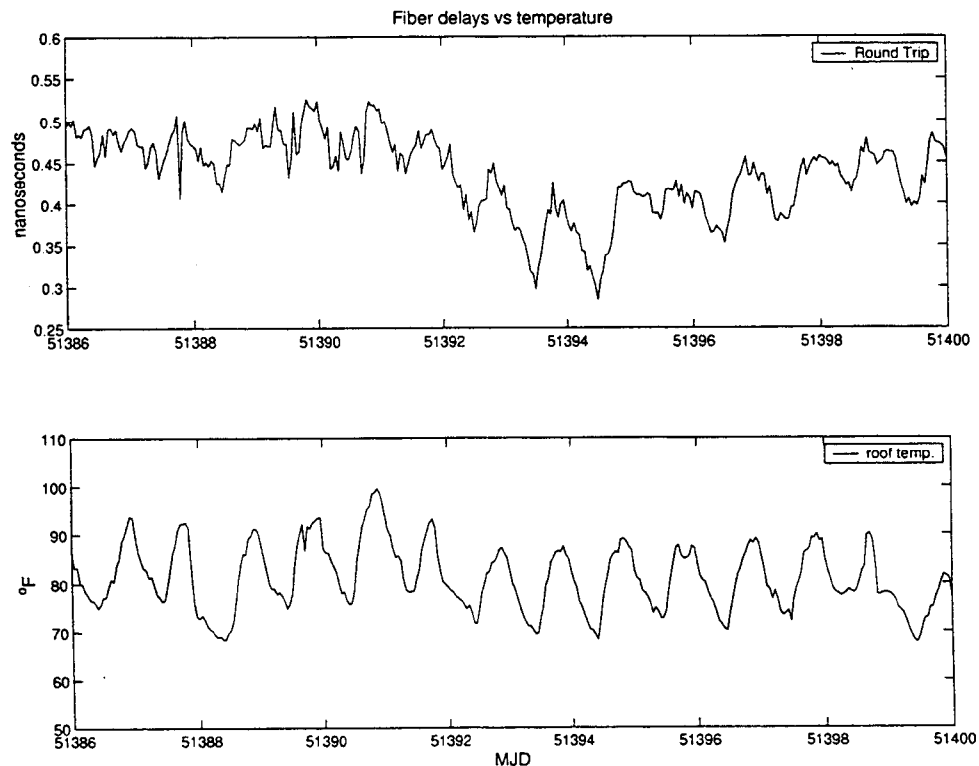


Figure 12. Round-trip path variations between USNO Buildings (top) and the exterior temperature (bottom).

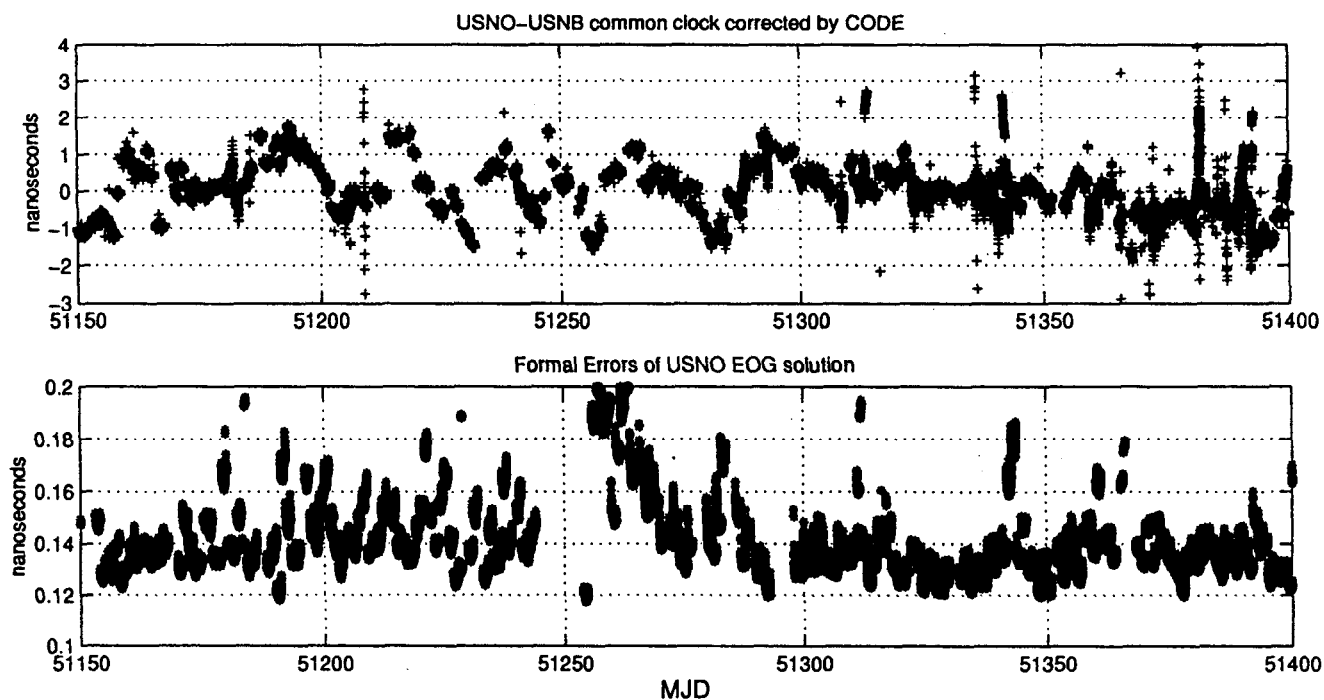


Figure 13. Upper plot is double difference of timing differences between USNO Bldgs. 52 and 78 measured by carrier phase and reduced by CODE/Bernese vs. those measured using LED-based fiber optics. Constants were removed to handle GPS receiver jumps just before MJDs 51038, 51051, and 51226. Lower plot is the formal error of the GIPSY computations.

## Questions and Answers

PETER WOLF (BIPM): This is just a detail. You said that at at some point that you cheated for phases, you called it; you smoothed over date boundaries. That means you just adjusted between 2 days, the jump, basically.

DEMETRIOS MATSAKIS (USNO): What I actually did was convert everything to frequencies and then throw out the frequency that crossed the day boundary.

GERARD PETIT (BIPM): By doing so, don't you extend the short-term stability of the maser to longer term? By removing the differences at the boundary?

MATSAKIS: Well, that is just a difference between two 5-minute points. So basically, I'm assuming that the maser is constant over those 10 minutes, constant in rate and drift. If a maser did something very funny right there and it just happened to correspond to midnight, that would certainly be hidden.

But actually the Percival algorithm washes all those problems away anyway.

DAVID ALLAN (Allan's Time): Had you looked at JPL-calibrated round-trip fiber optic? They're doing, I think, 30 picoseconds at the antenna with respect to their masers, using that technique for comparing the two.

MATSAKIS: I'm aware of them. I'm not aware of the bill. It's how much do we want to spend. And as we get more into carrier phase, the kind of money those kinds of systems involve gets less and less, figuratively speaking.

We also, of course, have plans in 5 or 10 years to have a new building which will house all our clocks. And all the fiber-optic questions will go away. Although it's an incredible annoyance for us to deal with fiber optics, the reason I brought it up was because I was more interested at looking at what short-baseline carrier phase does. And to show that the fiber optics, although they were a problem, were less of a problem than the carrier phase was itself.